

Nitric Oxide (NO) Traffic in Endothelial NO Synthase

EVIDENCE FOR A NEW NO BINDING SITE DEPENDENT ON TETRAHYDROBIOPTERIN?*

Received for publication, September 7, 2001, and in revised form, November 20, 2001
Published, JBC Papers in Press, November 21, 2001, DOI 10.1074/jbc.M108657200

Anny Slama-Schwok^{‡§}, Michel Nègrerie[‡], Vladimir Berka[¶], Jean-Christophe Lambry[‡],
Ah-Lim Tsai[¶], Marten H. Vos[‡], and Jean-Louis Martin[‡]

From the [‡]Laboratory for Optics and Biosciences, INSERM U451, CNRS Unité Mixte de Recherche 7645, Ecole Polytechnique, 91128 Palaiseau, France and the [¶]UTHTMC Medical School Division of Hematology, Houston, Texas 77030

Nitric oxide (NO) traffic within the reduced ferrous-nitrosyl complex of endothelial nitric-oxide synthase (eNOS) has been studied by ultrafast time-resolved absorption spectroscopy. In the presence of tetrahydrobiopterin, the rate of NO rebinding to the heme upon photodissociation depends on the NO concentration. The time scale of this process, picoseconds to nanoseconds, precludes a diffusion from the solution toward the protein medium, and altogether the data point at a new NO binding site within the protein. Comparison of the kinetics of pterin-bound and -depleted eNOS points out that the existence of this new site depends on the presence of tetrahydrobiopterin. The new non-heme site may act as a “doorstep” to the heme pocket and control NO escape from eNOS.

Nitric oxide (NO)¹ is produced from L-arginine in the vascular endothelium by the endothelial isoform of nitric-oxide synthase, eNOS. NO production is crucial in the control of vascular tone, arterial pressure, smooth muscle cell proliferation, and platelet adhesion to the endothelial surface. NOS catalyzes the formation of NO and L-citrulline from L-arginine in the presence of oxygen and NADPH (1). The active protein is a homodimer (2). Upon Ca²⁺/calmodulin binding, the FAD of the reductase domain transfers reducing equivalents from NADPH to FMN, which then reduces the heme iron located in the oxygenase domain. This domain also includes binding sites for the substrate, L-arginine, and the cofactor, tetrahydrobiopterin (BH₄). The cofactor BH₄ is required for full activity of all NOS isoforms. Reconstitution of holoenzyme activity and BH₄ binding requires the presence of glutathione, necessary to reduce an oxidized cysteine (3). BH₄ binds at the edge of, and perpendicular to, the heme plane through an extensive network of hydrogen bonds (4–6).

In this report, we focus on the effect of NO concentration on the dynamics of NO released from the ferrous-nitrosyl complex, Fe(II)-NO (7), and its potential role in controlling NO release from NOS. The ultrafast rebinding of a dissociated NO molecule to the eNOS heme site, a process called geminate recom-

ination, involves NO molecules that do not escape into the solvent. The kinetics of this rebinding are very sensitive to the environment of the heme. This ligand rebinding is studied at various NO concentrations.

In this work, we show that varying the NO to the protein ratio induces changes in the geminate recombination rate for eNOS possessing bound BH₄. In contrast, the rate of NO rebinding to BH₄-depleted eNOS was independent of NO concentration and much slower than in the presence of the cofactor. Our data strongly suggest the existence of a new non-heme binding site for NO that depends on the presence of BH₄.

EXPERIMENTAL PROCEDURES

Materials—L-Arginine, β-NADPH (99.8% purity), (6R)5,6,7,8-tetrahydrobiopterin (BH₄), and calmodulin, as well as other chemicals used for buffer preparations, were purchased from Sigma. Diluted NO gas at 1 and 10% (v/v) in nitrogen and argon, respectively, and high purity argon (99.9999%) were obtained from Air Products and Chemicals, Allentown, PA.

Expression and Purification of eNOS—Recombinant human eNOS was prepared using the baculovirus expression system in sf9 cells with replenishment of sepiapterin as described previously (8, 9). The purified enzyme containing 60% BH₄ was stored in liquid nitrogen in buffer containing 50 mM Tris-HCl at pH 7.5, 10% glycerol, and 0.15 M NaCl. BH₄-depleted bovine eNOS was prepared from an *Escherichia coli* expression system as described previously (7). The preparation of BH₄-bound eNOS prepared from *E. coli* containing 70% BH₄ was described previously (10).

Preparation of Samples for Spectroscopy—70 μl of eNOS (60 μM) were mixed to a 20-μl solution containing 10 mM L-arginine, 500 μM CaCl₂, 400 μM calmodulin, and 20 mg/ml 1,2-diheptanoyl-*sn*-glycero-3-phosphotidylcholine (DHPC) in a 1-mm optical path quartz cuvette kept in an ice bath. The cuvette was sealed with a rubber stopper and degassed by repetitive cycles of vacuum and argon purging. 10 μl of air-free NADPH (20 mM) was then added to the eNOS solution using a gas-tight syringe (Dynamech), followed by another cycle of vacuum and argon purging. The completion of the reduction step was achieved in about 10–15 min as measured by the absorption spectra. 1% NO gas was then introduced in the cell using a gas train. When lower NO concentrations were used, the required volume of NO at 1% was added to the cell at a constant total pressure of 1.3 bar by means of an airtight syringe. The cell was gently shaken for 20 min at (3 ± 1) °C. This procedure assured an efficient equilibration of NO between the liquid and gas phases. The absorption spectrum was subsequently recorded.

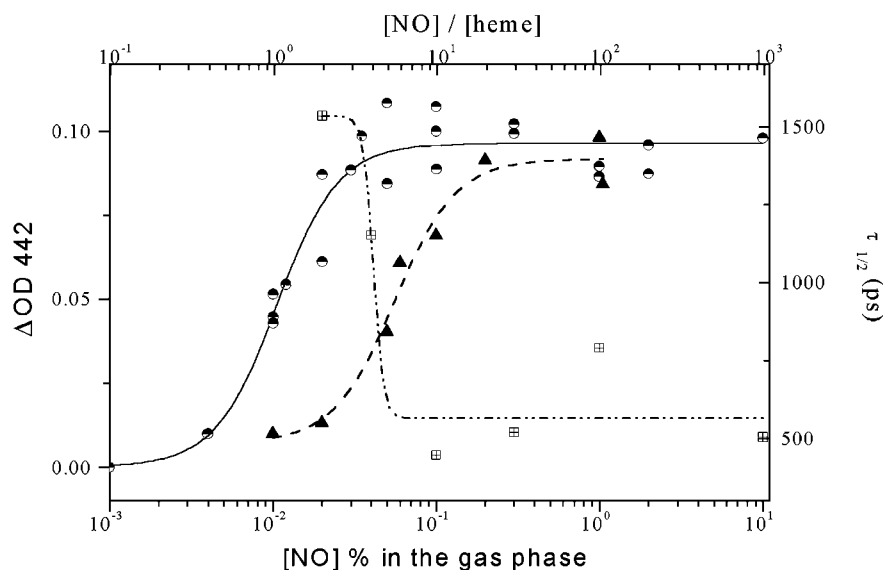
Time-resolved Spectroscopy—Time-resolved spectroscopy was performed with the 30-Hz pump-probe laser system described previously (11). The cell was placed in a thermostated cell holder at (20.0 ± 0.5) °C. Photodissociation of NO was achieved using an excitation pulse centered at 563 nm with a 40-femtosecond duration. The wavelength of this pump pulse matches the α-band of NO-liganded eNOS. The transient spectrum obtained after a variable delay was probed with a white light continuum pulse, whose group velocity dispersion was minimized at 410 nm by a set of prisms. 20 to 40 scans were recorded in durations of 200 ps and 4 ns and averaged (in such scan, each time point of a kinetic trace at a given wavelength represents the average of 300 laser shots). In some experiments, the dwell time was increased from 10 to 30 s, and

* This work was supported in part by National Institutes of Health Grant GM 56818 (to A. L. T.). The costs of publication of this article were defrayed in part by the payment of page charges. This article must therefore be hereby marked “advertisement” in accordance with 18 U.S.C. Section 1734 solely to indicate this fact.

§ To whom correspondence should be addressed. Tel.: 33-1-69333101; Fax: 33-1-69333017; E-mail: anny.schwok@polytechnique.fr.

¹ The abbreviations used are: NO, nitric oxide; NOS, NO synthase; eNOS, endothelial NOS; nNOS, neuronal NOS; iNOS, inducible NOS; SVD, singular value decomposition; DHPC, 1,2-diheptanoyl-*sn*-glycero-3-phosphotidylcholine.

FIG. 1. Comparison of the binding isotherm of NO to reduced eNOS heme and the NO binding curve of the new non-heme site. Left scale and circles, the absorbance difference between NO-bound and reduced eNOS containing 60% BH₄ monitored at 442 nm was plotted as a function of the NO concentration in the gas phase; solid line, sigmoidal fit to the experimental data; upper scale, the ratio of the total NO concentration over the heme concentration is calculated at [NO] = 1 × 10⁻³ – 10% in the gas phase; left scale and triangles, absorbance difference between NO-bound and reduced BH₄-depleted eNOS; right scale and squares, experimental half-life, τ_{1/2}, as a function of NO concentration in BH₄-bound eNOS; dashed line, sigmoidal fit to the experimental data. Sample conditions were as follows: [eNOS] = 50 μM, [NADPH] = [L-arginine] = 2 mM, 80 μM calmodulin, 100 μM CaCl₂ in 50 mM Tris-HCl buffer at pH 7.5 containing 10% glycerol and 0.15 M NaCl. Measurements were made at 20 °C.



20 scans were averaged at a few time points to improve the signal to noise ratio in transient spectra. Analysis of the data was performed by singular value decomposition (SVD) of the time-wavelength matrix (12). The kinetics associated with the SVD components having the highest singular values were fit with a minimum number of exponentials. Reduced and carbon monoxide-bound myoglobin and hemin were monitored in the same conditions and used as references of flat kinetics in the time scales of 200 ps to 4 ns (13).

RESULTS

Binding Isotherm of NO to Reduced eNOS—Binding of NO to reduced eNOS induces an absorption increase at 436 nm of the Soret band and a simultaneous decrease at 410 nm that corresponds to the absorption maximum of the reduced unliganded heme. Spectral changes are also observed in the Q-bands, as shown by a progressive red shift of the 560-nm band to 569 nm upon NO addition. Fig. 1 shows the absorption changes for the ferrous-NO complex monitored at $\lambda = 442$ nm as a function of the concentration of added NO using BH₄-bound eNOS. ΔOD increased with added NO in the range of 0.001 to 0.03% and then leveled off. The same ΔOD value was obtained varying NO concentrations from 0.1 to 10%. The data fit a sigmoidal curve, which indicated that NO binding reached saturation at about 0.03–0.04% NO. This saturation level of 0.03 to 0.04% corresponds to 0.6 μM NO in solution, a much lower concentration than that of reduced eNOS. However it is unlikely that the liquid-gas phase equilibrium of NO is unperturbed by the presence of eNOS. The protein could modify the NO distribution between liquid and gas phases, depleting NO from the gas phase because of its high affinity for NO. If one assumes that each NO added is transferred to the solution because of this depletion, then the plateau is reached between three and four NO bound per heme (Fig. 1, upper scale) and remains constant within experimental error up to 1000 NO molecules per heme.

Fig. 1 also presents the difference maximum, ΔOD 442 nm, as a function of added NO in the gas phase using BH₄-depleted eNOS. The data fit a sigmoidal curve with a plateau reached at about 0.2% NO. The comparison between isothermal binding of NO by BH₄-depleted eNOS and eNOS containing BH₄ clearly shows that NO binds more tightly to the latter; the half-saturation is reached at 0.055 and 0.01% NO, respectively.

NO Recombination to the BH₄-bound Heme at [NO] ≥ 0.3%—The recombination of diatomic ligands, such as NO, with the heme prosthetic group in proteins generally occurred in non-monoexponential phases. The fast phase of geminate recombina-

tion involved the rebinding of NO molecules prior to their escape from the protein into the solvent. This phase generally took place on the submicrosecond time scale and can be coupled to protein dynamics known to occur on such time scales (14). The slower phase involved the recombination of ligands after their escape into the solution. It followed bimolecular kinetics and occurred on the millisecond time scale for the protein and ligand concentrations usually studied. Our experiments probed the faster geminate recombination of NO with the heme, a step contributing to both on and off rates.

Excitation of NO-bound eNOS with a laser pulse induced NO dissociation from the heme. A second pulse then allowed to probe the spectral changes associated with NO rebinding to the heme. These spectral changes correspond to a difference between spectra collected at a given time delay, t , after photodissociation. Typical transient spectra are shown in Fig. 2. The spectra recorded within the first few picoseconds included a contribution of the excited state absorption, the decay of which was clearly seen around 460 nm. The spectra obtained at 240 ps and 3 ns presented a maximum at 406 nm and a minimum at 436 nm, with an isosbestic point at 425 nm. These spectral features are characteristic of the reduced unliganded eNOS, because they are also found in the difference equilibrium spectrum between reduced eNOS and NO-bound protein (Fig. 2).

Kinetics of NO rebinding to the heme at 1.5% NO are characterized by a non-single exponential behavior including a fast phase occurring in the picosecond regime and a slow phase taking place in the ns time scale (Fig. 2). The transient absorption spectra recorded at 50 ps and 4 ns exhibited the same line shape, with the latter having a smaller amplitude. This implies that one monitored the decay of the same species in two phases. Accordingly, it appeared as a single and largest component in an SVD analysis. At 0.3% NO concentrations, the fit of the kinetics associated with this SVD component yielded three exponential terms, $\tau_1 = (32 \pm 9)$ ps, $\tau_2 = (0.3 \pm 0.1)$ ns, and $\tau_3 = (3.7 \pm 0.3)$ ns, and a non-decaying phase as shown in Fig. 3, curves *c* and *d*. The kinetic parameters are summarized in Table I. The kinetics were identical within experimental error at NO concentrations ranging from 0.3 to 10% (Table I).

Recombination of NO at Concentrations below [NO] = 0.3% Using BH₄-bound eNOS—The recombination kinetics clearly depended on NO concentration below [NO] = 0.3%. Fig. 3 shows that the geminate recombination rate was slower in both

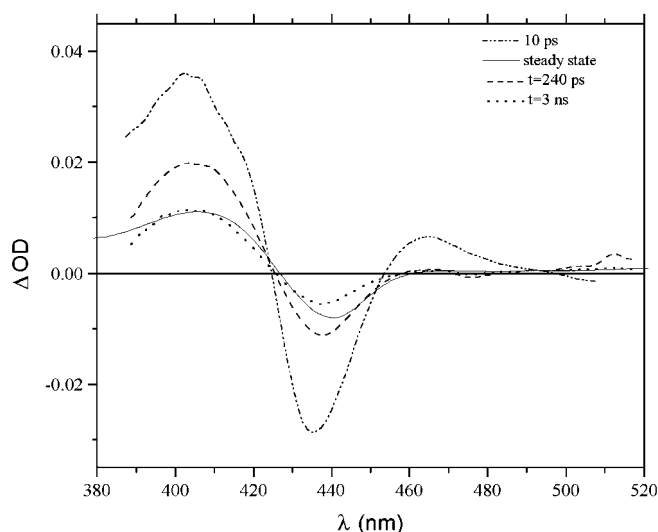


FIG. 2. Transient spectrum after NO photodissociation from reduced eNOS in the presence of $[\text{NO}] = 1.5\%$ in the gas phase. The raw transient spectra were monitored at 10 ps (dashed and dotted line), 240 ps (dashed line), 3 ns (dotted line) and steady state absorption difference between reduced eNOS and NO bound spectra (solid line). Experimental conditions are the same as in Fig. 1.

the picosecond and nanosecond time ranges at $[\text{NO}] = 0.02\%$ (curve *a*) than at $[\text{NO}] = 0.3\%$ (see curve *c* and Table I). This lower rate of rebinding resulted in a higher percentage of non-liganded NOS remaining after $t = 3$ ns. Intermediate kinetics were obtained near saturation, $[\text{NO}] = 0.1\%$; see curve *b*. Kinetics monitored at $[\text{NO}] = 0.04\%$ are fitted by two exponentials with similar time constants to those obtained at $[\text{NO}] = 0.02\%$ although the pre-exponential (amplitude) terms differ (Table I).

Kinetics of NO Rebinding to the Heme in BH_4 -depleted eNOS; Comparison with BH_4 -bound eNOS—Fig. 4 shows that NO rebinding to the heme occurred in a non-single exponential steps characterized by a fast phase occurring in picoseconds and a slow phase taking place in the nanosecond time scale. The kinetics was independent of NO concentration in the range of 0.1 to 10%. The data can be fit by two exponential terms and a non-decaying phase, $\tau_1 = (90 \pm 30)$ ps and $\tau_2 = (1.2 \pm 0.3)$ ns (see Table II). Similar kinetics was also recorded at 0.05% NO and yielded similar lifetimes but had a higher uncertainty because of low signal to noise ratio.

This behavior contrasted the clear NO dependence shown in Fig. 3 for BH_4 -bound eNOS. This difference between BH_4 -depleted and BH_4 -bound eNOS occurred at similar NO concentrations. Fig. 4 also presents kinetics of NO recombination to the heme in BH_4 -bound eNOS. It is clearly seen that the geminate recombination was much faster in the presence of BH_4 than in its absence. This contrasts with the lack of effect of BH_4 on the geminate rebinding of NO to the ferric eNOS (7).

Comparison of BH_4 -bound eNOS from *E. coli* and Baculovirus—As shown in Fig. 3 and Fig. 4, BH_4 -bound and -depleted eNOS differ in the NO dependence of NO rebinding kinetics. However, the eNOS samples differ in their expression system (from Sf9 and *E. coli*, respectively). The experiments were thus also performed with BH_4 -bound eNOS prepared by the *E. coli* expression system to ensure that the NO dependence of the rebinding kinetics could not be because of some structural changes between the two preparations. The inset of Fig. 3 shows that a much slower kinetics is obtained at 0.02% NO than that recorded at 1.5% NO. Thus, the sample prepared in the *E. coli* system follows qualitatively the same trend as described previously for the baculovirus expression (Fig. 3)

with the NO concentration effect on NO rebinding kinetics observed in the presence of the pterin cofactor but not in its absence of BH_4 .

DISCUSSION

Evidence for a New Non-heme NO Binding Site in eNOS—Our transient absorption experiments probed the recombination kinetics of NO with the heme on a time scale where only intraprotein processes are relevant. The picosecond phase is due to the rebinding of NO that did not escape the heme pocket after photodissociation and is presumably activationless, whereas the nanosecond phase reflects rebinding of ligands that have overcome an energy barrier (7, 15). Recombination of photodissociated NO took place in the picosecond to nanosecond time scale, which was not long enough to allow diffusion of NO molecules from the bulk solution toward the protein interior. Taking the on-rate of NO binding to the ferrous eNOS, $k_{\text{on}} = 1.1 \times 10^6 \text{ M}^{-1} \cdot \text{s}^{-1}$ (16), assuming an NO concentration of 0.4 μM at $[\text{NO}] = 0.02\%$, there should only be an effect of bulk NO concentration in the time range of hundreds of milliseconds, much slower than the process we were measuring. Hence the NO concentration effect must arise from diffusion and/or transfer processes within the protein.

Several hypotheses may explain the dependence of the rebinding kinetics on NO concentration. Three possibilities need to be considered. The first deals with the heterogeneity of the enzyme in terms of BH_4 content, the second one has to do with a new non-heme site that binds NO. This site may compete with the heme for NO binding or may modify NO trajectory by steric effects, and in the third hypothesis, there is an NO-dependent regulatory site that may be electronically coupled with the heme via BH_4 and thus lower the energy barrier for recombination.

Heterogeneity of the Enzyme—First, we have to consider that our BH_4 -containing sample is actually composed of a heterogeneous population with respect to BH_4 content; 60% of the protein contains BH_4 , and the remaining 40% is depleted of the cofactor. Table I and Table II show that NO rebinding to BH_4 -depleted heme is slower than that in its presence. Thus, the slower rate at low NO concentration obtained with eNOS containing 60% BH_4 could be because of the preferential NO rebinding to BH_4 -depleted heme. This held true if the affinity of NO for BH_4 -depleted heme was higher than for BH_4 -bound protein. However, Fig. 1 shows that the inverse situation occurs; the affinity of NO for BH_4 -depleted eNOS is lower than for BH_4 -bound protein. Thus, the heterogeneous population seems unlikely to be the origin of the NO dependence of the kinetics.

New NO Binding Site—Second, we discuss the availability of a new NO binding site near the heme as a target for binding. An estimate for the affinity of this site for NO is given by the plot of the apparent half-life time, $\tau_{1/2}$ (Fig. 1), as a function of NO concentration in the range 0.02 to 10% (NO concentrations below 0.02% yielded a signal too small to obtain reliable kinetics). An apparent K_D for this non-heme site is estimated at $[\text{NO}] = 0.04\%$ corresponding to four NO per protein compared with that of the heme in the same conditions $[\text{NO}] = 0.01\%$, i.e. one NO per protein. The transfer of NO from the non-heme site to the heme may thus be facilitated by its lower affinity for NO compared with that of the reduced heme.

Scheme 1A assumes that the NO molecules dissociated from the heme by the laser pulse may recombine either to the heme or to the new site. The kinetics of the picosecond rebinding fraction to the heme would become faster in the presence of this site than if the heme was the only recombination site and would introduce a dependence on NO concentration, reflecting the occupancy of the non-heme site. Once this new site is fully

FIG. 3. Effect of NO concentration on the decay of the main SVD kinetic component using BH₄-bound eNOS. Normalized experimental decay of the main SVD component obtained in the time windows of 200 ps and 4 ns and fitted decay by 2 or 3 exponential terms using the sf9 expression system (Table I) are shown. Experimental conditions are the same as in Fig. 1; squares, [NO] = 0.02%; circles, [NO] = 0.1%; triangles, [NO] = 0.3%; and stars, [NO] = 10%. Inset, normalized experimental decay of the main SVD component using the BH₄-bound eNOS prepared from *E. coli* at 0.02% NO, 1 and squares; and at 1.5% NO, 2 and circles.

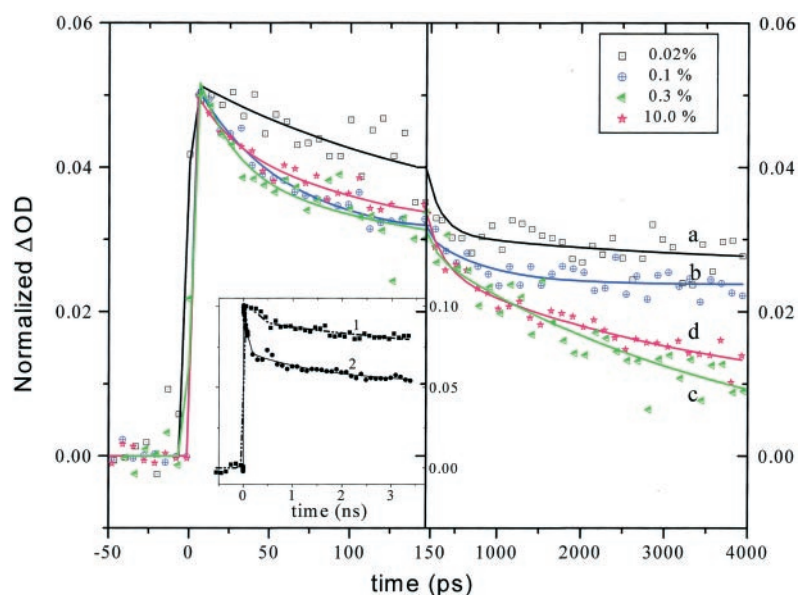


TABLE I
Kinetic parameters obtained from BH₄-bound eNOS

Parameters obtained by fitting the kinetics associated with the main SVD component. [eNOS] = 50 μM containing 60% BH₄, 2 mM NADPH, 2 mM L-arginine in Tris buffer at pH 7.5, 2.1 mM DHPC at 20 °C. The model used for fitting consists of a sum of exponentials and a constant term.

NO	[NO]/[Fe(II)] ^a	τ ₁	A ₁ ^b	τ ₂	A ₂ ^b	τ ₃	A ₃ ^b	A ₄ ^c
%		ps		ps		ns		
0.02	2	180	0.32			≥3.1	0.68	
0.04	4	120	0.54			≥2.9	0.46	
0.1	10	44	0.35	390	0.20	4.1	0.25	0.20
0.3	30	22	0.29	120	0.19	3.9	0.49	0.03
1.0	100	40	0.24	400	0.19	3.7	0.44	0.13
10	1000	21	0.18	200	0.31	3.3	0.37	0.14

^a Molar ratio of the total NO amount (aqueous and gaseous phases) over the heme amount.

^b Relative amplitude, A₁ + A₂ + A₃ + A₄ = 1, not including the amplitude of the transient due to the excited state.

^c Amplitude of the constant component (τ₄ >> 4 ns).

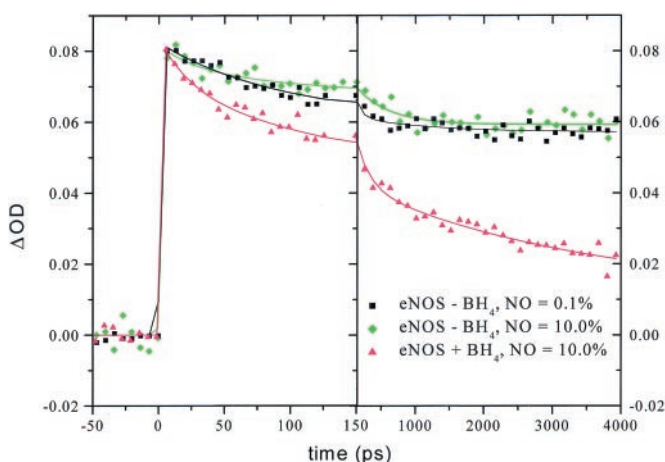


FIG. 4. Effect of NO concentration on the decay of the main SVD kinetic component using BH₄-depleted eNOS. Squares, [NO] = 0.1%; diamonds, [NO] = 10%; the decay of BH₄-bound eNOS in the presence of 10% NO is also represented for comparison (triangles). Experimental conditions are the same as in Fig. 1.

saturated with NO, the kinetics became independent of NO concentration, because the dissociated NO has only one target left, the heme.

Alternatively, the accommodation of a second NO bound to the non-heme site near the heme may limit the volume in which the released NO can move (the heme pocket) and hence increase the probability of colliding with the heme iron (17). NO rebinding to the heme is here purely geminate. However,

the present hypothesis implies a close proximity between the heme and the second site. Our data indicate that this site has to be located close enough to the heme to allow such a rebinding to occur within hundreds of picoseconds to nanoseconds. Considering the reported values for CO and oxygen diffusion coefficients within proteins, ranging between 10⁻⁷ and 10⁻¹¹ cm²/s, one can crudely estimate that the distance between the new NO site and the heme should not exceed ~10 Å (18, 19). Such a distance of ~10 Å may be too large to hinder NO recombination to the heme by steric effects.

We now turn to the potential nature of the proposed binding site. One possibility is that NO binds to metal ions such as iron and copper. For instance, Marletta and co-workers (20) have shown that the inducible and neuronal isoforms of NOS (iNOS and nNOS) can bind one equivalent of non-heme iron per monomer that stimulates the catalytic activity. Based on the well established iron-BH₄-coupled hydroxylation, these authors proposed the amino acids Asp-650, His-692, and His-652 (the numbering refers to nNOS), which lie above the heme plane in proximity to the C4a pterin edge, to form the iron binding site in nNOS (20). However, x-ray and mutation studies failed to reveal metal binding in the vicinity of the C4a position of BH₄ (4–6). Other transition metals have been shown to interact with NOS, and in particular Cu²⁺ and Zn²⁺ inhibit NOS catalysis through an interaction with the reductase domain (21, 22). These metal centers should be irrelevant for our geminate rebinding of NO.

Another possibility is that cysteine residues close to the heme and BH₄ act as an NO binding site (cysteines constitute

TABLE II
Kinetic parameters obtained from BH_4 -absent eNOS

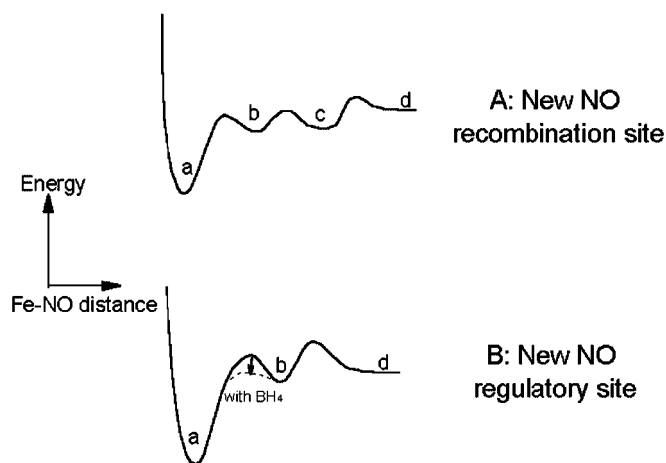
Parameters obtained by fitting the kinetics associated with the main SVD component. [eNOS] = 70 μ M depleted in BH_4 , 2 mM NADPH, 2 mM L-arginine in Tris buffer at pH 7.5, 2.1 mM DHPC at 20 °C. The model used for fitting consists of a sum of exponentials and a constant term.

NO	[NO]/[Fe(II)] ^a	τ_1	A_1^b	τ_2	A_2^b	A_3^{bc}
%		ps		ns		
0.05	5	121	0.18	1.2	0.09	0.73
0.1	10	88	0.14	1.1	0.16	0.70
0.2	20	121	0.08	1.4	0.36	0.56
1.0	100	72	0.20	1.5	0.25	0.55
10	1000	66	0.14	0.9	0.13	0.73

^a Molar ratio of the total NO amount (aqueous and gaseous phases) over the heme amount.

^b Relative amplitude, $A_1 + A_2 + A_3 = 1$, not including the amplitude of the transient due to the excited state.

^c Amplitude of the constant component ($\tau_3 \gg 4$ ns).



SCHEME 1. Possible explanations for the effect of NO concentration on the kinetics of NO rebinding to the heme in the presence of BH_4 . A presents the model of a new NO binding site near the heme pocket; a, b, c, and d represent, respectively, the heme, the heme pocket, the new site, and the space outside the protein. B shows the hypothesis of a new regulatory site that lowers the energy barrier between the heme and the heme pocket in the presence of BH_4 .

one of the most probable NO targets besides metallic ions in the protein). One such residue is Cys-443 located 15 Å from the heme iron, which is probably too far from the heme to constitute the second NO site. Alternatively, this site could be a cysteine located in the reductase domain close to the heme pocket and to the BH_4 binding site. Two cysteine residues located in the reductase domain have been suggested to be important for BH_4 binding and activity (3). Work along these lines is in progress in our laboratory.

New NO Regulatory Site—The third hypothesis also involves a non-heme NO binding site as a regulatory element of NO evolution rather than a participant in the recombination. It assumes that the presence of this site lowers the activation energy barrier for recombination to the heme from the heme pocket (Scheme 1B). The filling of this site with NO progressively lowers the energy barrier for recombination that is truly geminate. Once this site is saturated with NO, the kinetics becomes independent on NO concentration. BH_4 rigidifying the heme could be one major reason to lower the energy barrier. To decrease the energy barrier, the new site has to be located close to the BH_4 binding site and is probably coupled to BH_4 and indirectly to the heme via hydrogen bonds between BH_4 and the heme. This would explain why the BH_4 cofactor has to be present for an NO concentration dependence on the recombination to exist. The existence of such a coupling is also consistent with BH_4 affecting the heme midpoint potential (23). This coupling is also likely to affect the rebinding kinetics in the hundreds of picoseconds to nanoseconds range, because it may directly control the heme reactivity. In this hypothesis, the

nature of the regulatory site may be, as suggested above, a cysteine residue or BH_4 itself (see below).

Importance of the Presence of Tetrahydrobiopterin in the Control of NO Traffic within eNOS—The binding isotherms of NO to BH_4 -bound and BH_4 -depleted eNOS are clearly shifted from one another (Fig. 1, inset). This implies a lower affinity of NO for the reduced heme in the absence of the cofactor, possibly because of a larger distance between the iron and L-arginine (24). The data of Fig. 4 and Table II clearly show the lack of NO dependence in BH_4 -depleted sample. This holds true for concentration from 0.1 to 10%. Thus, in this case, NO rebinding to the heme is purely geminate without any possible contribution of NO from another site in the protein except the heme. This contrasts with the kinetics obtained in the presence of BH_4 , in particular at the NO concentration of 0.1% for which the rate of decay is clearly intermediate between that obtained at 0.02 and 0.3 or 10% (Fig. 3). Thus, the existence of the new non-heme site depends on the presence of the pterin cofactor. Furthermore, the recombination is faster in the presence of BH_4 than in its absence especially at high NO concentrations (1–10%). This suggests that the cofactor controls NO traffic and/or release from the reduced protein. The presence of the cofactor may tighten the conformation of the reduced heme pocket. In contrast, BH_4 does not modify the rate of geminate recombination in the ferric enzyme (7), in agreement with the lack of conformational change observed in ferric eNOS with and without pterin by x-ray diffraction (4).

Relevance of the Non-heme Site to the Catalysis of eNOS—Catalysis by NOS is tightly regulated at the molecular level. During catalysis, NO exerts a feedback control on its own synthesis. The neuronal NO-synthase is regulated at the level of the Fe(II)-NO complex whereas in the inducible isoform iNOS, a Fe(III)-NO complex predominates under steady state catalysis (25–27). In contrast, NO feedback inhibition seems to have a smaller impact on the catalysis of the endothelial isoform (16) that we study. The latter authors suggested that, for this isoform, the rate of electron transfer from the reductase domain to the heme is rate-limiting. Indeed, the electron transfer rate and the catalytic activity are the lowest in eNOS compared with nNOS and iNOS (28). In addition, mutation studies showed that an autoregulatory loop in the reductase domain of eNOS and nNOS exerts autoinhibition of the electron transfer (29, 30). A possible explanation for the absence of ferrous and ferric nitrosyl complexes under steady state catalysis in the presence of L-arginine could be related to NO occupancy of the new non-heme site, irrespective of the iron oxidation state of eNOS. In other words, this site may act as an NO “reservoir” or as an entry/exit gate to the heme pocket of eNOS.

REFERENCES

1. Stuehr, D. J. (1999) *Biochim. Biophys. Acta* **1411**, 217–230
2. Siddhanta, U., Presta, A., Fan, B., Wolan, D., Rousseau, D. L., and Stuehr, D. J. (1998) *J. Biol. Chem.* **273**, 18950–18958
3. Rusche, K. M., and Marletta, M. A. (2001) *J. Biol. Chem.* **276**, 421–427

4. Raman, C. S., Li, H., Martásek, P., Král, V., Masters, B. S. S., and Poulos, T. L. (1998) *Cell* **95**, 939–950
5. Fischmann, T. O., Hruza, A., Niu, X. D., Fossetta, J. D., Lunn, C. A., Dolphin, E., Prongay, A. J., Reichert, P., Lundell, D. J., Narula, S. K., and Weber, P. C. (1999) *Nat. Struct. Biol.* **6**, 233–242
6. Crane, B. R., Arvai, A. S., Gosh, S., Getzoff, E. D., Stuehr, D. J., and Tainer, J. A. (2000) *Biochemistry* **39**, 4608–4621
7. Négrerie, M., Berka, V., Vos, M. H., Lieble, U., Lambry, J.-C., Tsai, A.-L., and Martin, J.-L. (1999) *J. Biol. Chem.* **274**, 24694–24702
8. Chen, P.-F., Tsai, A.-L., Berka, V., and Wu, K. K. (1996) *J. Biol. Chem.* **271**, 14631–14635
9. Berka, V., Chen, P.-F., and Tsai, A.-L. (1996) *J. Biol. Chem.* **271**, 33293–33300
10. Berka, V., and Tsai, A.-L. (2000) *Biochemistry* **39**, 9373–9383
11. Martin, J.-L., and Vos, M. H. (1992) *Annu. Rev. Biophys. Biomol. Struct.* **21**, 199–222
12. Press, W. H., Teukolsky, S. A., Vetterling, W. T., and Flannery, B. P. (1988) *Numerical Recipes*. Cambridge University Press, Cambridge, UK
13. Petrich, J. W., Poyat, C., and Martin, J.-L. (1988) *Biochemistry* **27**, 4049–4060
14. Ansari, A., Jones, C. M., Henry, E. R., Hofrichter, J., and Eaton, W. A. (1994) *Biochemistry* **33**, 5128–5145
15. Henry, E. H., Eaton, W. A., and Hochstasser, R. M. (1986) *Proc. Natl. Acad. Sci. U. S. A.* **83**, 8982–8986
16. Abu-Soud, H. M., Ichimori, K., Presta, A., and Stuehr, D. J. (2000) *J. Biol. Chem.* **275**, 17349–17357
17. Vos, M. H., Lipowski, G., Lambry, J.-C., Martin, J.-L., and Liebl, U. (2001) *Biochemistry*, **40**, 7806–7811
18. Marden, M. C. (1982) *Eur. J. Biochem.* **128**, 399–404
19. Carrero, J., Jameson, D. M., and Gratton, E. (1995) *Biophys. Chem.* **54**, 143–154
20. Perry, J. M., and Marletta, M. A. (1998) *Proc. Natl. Acad. Sci. U. S. A.* **95**, 11101–11106
21. Persechini, A., McMillan, K., and Masters, B. S. (1995) *Biochemistry* **34**, 15091–15095
22. Perry, J. M., Zhao, Y., and Marletta, M. A. (2000) *J. Biol. Chem.* **275**, 14070–14076
23. Presta, A., Weber-Main, A. M., Stankovich, M. T., and Stuehr, D. J. (1998) *J. Am. Chem. Soc.* **120**, 9460–9465
24. Li, H., Raman, C. S., Martásek, P., Masters, B. S. S., and Poulos, T. L. (2001) *Biochemistry* **40**, 5399–5406
25. Abu-Soud, H. M., Gachhui, R., Raushel, F. M., and Stuehr, D. J. (1995) *J. Biol. Chem.* **272**, 17349–17353
26. Abu-Soud, H. M., Wu, C., Gosh, D. K., and Stuehr, D. J. (1998) *Biochemistry* **37**, 3777–3786
27. Hurschman, A. R., Krebs, C., Edmondson, D. E., Huynh, B. H. and Marletta, M. A. (1999) *Biochemistry* **38**, 15689–15696
28. Miller, R. T., Martásek, P., Omura, T., and Masters, B. S. (1999) *Biochem. Biophys. Res. Com.* **265**, 184–188
29. Nishida, C. R., and Ortiz de Montellano, P. R. (1999) *J. Biol. Chem.* **274**, 14692–14698
30. Chen, P. F., and Wu, K. K. (2000) *J. Biol. Chem.* **275**, 13155–13163